2E1-3

High speed noncontact acoustic inspection method using sound source mounted type UAV for the outer wall inspection

外壁点検のための音源搭載型 UAV を用いた
高速非接触音響探査法

Tsuneyoshi Sugimoto[1†], Kazuko Sugimoto[1], Itsuki Uechi[1], Noriyuki Utagawa[2] and Chitose Kuroda[2] ([1]Grad. School Eng., Toin Univ. of Yokohama, [2]Technical Research Institute, SatoKogyo Co., Ltd.)

杉本恒美 [1†]，杉本和子 [1]，上地樹 [1]，歌川紀之 [2]，黒田千歳 [2] （[1] 桐蔭横浜大院 工, [2] 佐藤工業㈱・技術研究所）

1. Introduction

As a non-destructive testing of concrete, we have studied noncontact acoustic inspection method using acoustic irradiation induced vibration and a laser Doppler vibrometer[1-3]. In our measurement, a long-range acoustic device (LRAD) as a sound source and a scanning laser Doppler vibrometer (SLDV) were used. Using our method, non-destructive testing is possible not only for a tunnel with curved surface but also for a remote measurement of a bridge from a distance of more than 30 meters away, and shotcrete with uneven surface[4]. Meanwhile, in Japan, according to law, old buildings that have been 10 years old since construction are obliged to inspect the entire outer wall by hammering test etc. However, contact inspection like a hammering test requires a scaffolding, so the cost burden is heavy and it is not realistic. On the other hands, in our method, if a sound source is mounted on an unmanned aerial vehicle (UAV), outer wall of building is able to be measured. Compared with sound irradiation from a sound source on the ground, a sound source mounted on a UAV just faces to the wall and there becomes no problem of angle dependency of sound waves. Therefore, we examined the outer wall inspection by our noncontact acoustic inspection method using sound source mounted type UAV.

2. Sound source mounted type UAV and outer wall specimen

Fig.1 shows an external view of a sound source mounted UAV (prototype). The base body is DJI's Matrice 600 Pro, which is equipped with a flat speaker (FPS 1030M3F1R), a sighting laser pointer and a laser rangefinder on the underside of the aircraft. **Fig.2** shows the layout of the simulated defect sheet embedded in the outer wall specimen ($2 \times 1.6 \times 0.2$ m^3) manufactured for the verification experiment. The burial depth of the sheet is about 9 mm from the tile surface, assuming that the distance from the base material (concrete) to the upper surface of the tile is 10 mm (depending on the mortar thickness and the penetration thickness of the tile, foam sheet thickness : 1 mm, styrene sheet : 0.5 mm + double-sided tape : 0.5 mm). The size of one tile is about 45 × 95 mm^2. This time, the sound wave irradiation experiment from the UAV was performed on the upper two rows of simulated defects (defect size 50 to 200 mm^2) of the outer wall specimen due to the measurement time.

Fig.1. Sound source mounted type UAV.

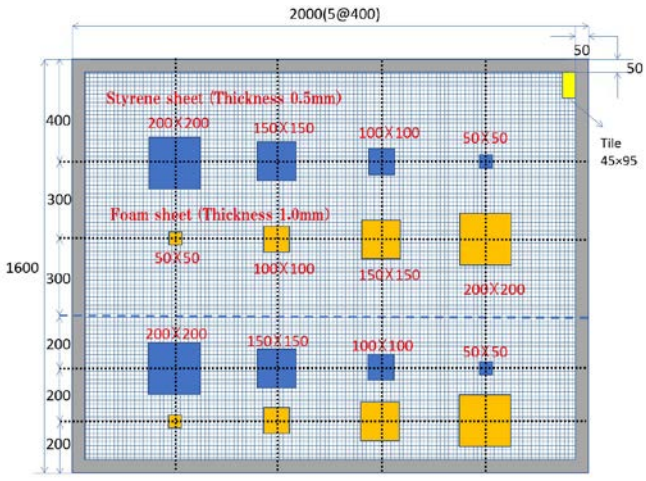

Fig.2. Arrangement of simulated defects of outer wall specimen. Styrene sheets and foamed sheets were used as simulated defects.

†tsugimot@toin.ac.jp

3. Acoustic irradiation experiment

3.1 Experimental setup

An experiment setup in the verification experiment is shown in **Fig.3**. A sound source mounted type UAV faced almost to the simulated defect position, and the distance to the outer wall specimen was about 1.6 to 1.7 m. As shown in the figure, the SLDV was subjected to vibration measurement at an angle of about 38° to 55° obliquely from a distance of about 2.4 to 3.4 m. The waveform used for acoustic irradiation induced vibration was a single tone burst wave, and two kinds of waveforms were created and used to match the flexural resonance frequency of the target defect. The first waveform was used when the frequency range was 0.5 to 4 kHz and the defect size was 100 to 200 mm^2. The second waveform is a single tone burst wave of 9 to 13 kHz and it was used when the defect size was 50 mm^2. Both waveforms have a modulation frequency of 100 Hz, an interval of 15 ms, and a pulse width of 5 ms. The sound pressure at the time of excitation was set to about 95 dB on the measurement target surface. Since the strong wind blows at the time of the experiment, the UAV does not actually fly but performs measurement in a state of being mounted on the rear part of the carrying vehicle.

3.2 Experimental result

Fig.4 shows an example of the imaging result based on the vibration energy ratio in the frequency band used. The frequency range for calculating the vibration energy ratio is 0.5 to 4 kHz when the size of the defect is 100 to 200 mm^2 and 9 to 13 kHz when it is 50 mm^2 according to the emission waveform. The number of measurement points was 121 (11 × 11), and the measurement time was about 9 minutes 11 seconds when the average was 5 times. The temperature at the time of measurement was about 10 °C for outdoor experiment. As can be seen from the figure, all defect sizes of 50 to 200 mm^2 are detected. Among these defects, 50 mm^2 defects have a flexural resonance frequency as high as 10 kHz or more, which is a difficult defect to be found by the hammering test.

4. Conclusion

We demonstrated that peeling defects of outer wall tiles can be detected by a method utilizing flexural resonance even with a small sound source that can be mounted on UAV. In addition, since it can be accessed in a state of facing the defective part, it is possible to simultaneously solve both angle dependency and environmental noise problem, which were problems of the conventional noncontact acoustic inspection method. Furthermore, since the influence of reflected waves is reduced because the position of the sound source is separated from the position of the LDV, higher Signal to Noise ratio can be expected with higher speed measurement.

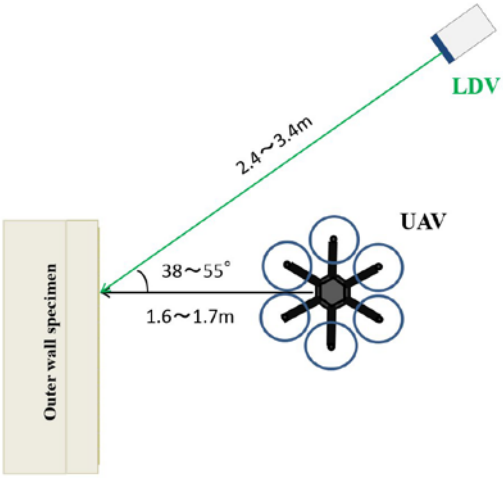

Fig.3. Experimental setup using UAV and LDV.

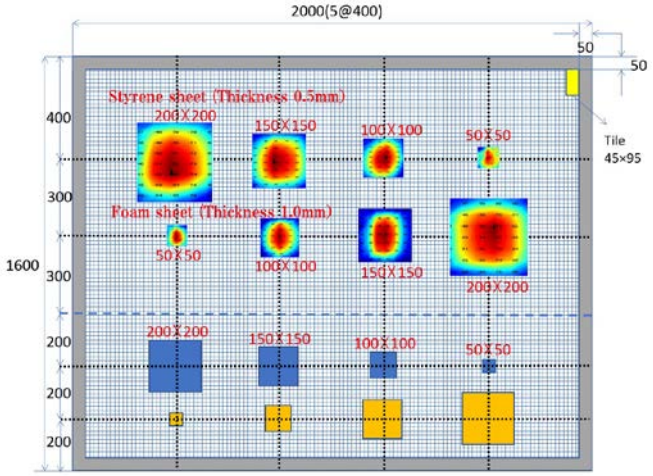

Fig.4. Experimental result using vibration energy ratio. All simulated defects can be detected.

Acknowledgment

This work was supported by MLIT Grant of Construction Technology R & D and JSPS KAKENHI Grant Number JP17K12991.

References

1. K. Katakura, R.Akamatsu, T.Sugimoto, *et al.*: Jpn. J. Appl. Phys. **53** (2014) 07KC15.
2. K.Sugimoto, R.Akamatsu, T.Sugimoto, *et al.*: Jpn. J. Appl. Phys. **54** (2015) 07HC15.
3. T.Sugimoto, K.Sugimoto, N.Utagawa, *et al.*: Jpn. J. Appl. Phys. **56** (2017) 07JC10.
4. K.Sugimoto, T.Sugimoto, N.Utagawa, C.Kuroda *et al.*: Jpn. J. Appl. Phys. **57** (2018) 07LC13.